Journal of Building Technology, 2024, Volume 6, Issue 2
DOI: 10.32629/jbt.v6i2.2579
ISSN Online: 2717-5103
ISSN Print: 2705-1390

Thermal Behaviour of Hydrofugated Plaster Block Masonry with Variation of Coating Thickness

José Reginaldo de Arruda Cavalcanti[1], Pedro Igor Bezerra Batista[1], Yêda Vieira Póvoas[1], Joaquin Humberto Aquino Rocha[2]

1. Polytechnic School of Pernambuco, University of Pernambuco, 50720-001, Recife, Brazil.
2. School of Technology, Universidad Privada del Valle, Tiquipaya, Bolivia.

Abstract: The objective of this research is to analyze the influence of ceramic coating, simulating the external side, and plaster with different thicknesses, simulating the internal side of a prototype of solid water-repellent gypsum block masonry, aiming to improve the thermal performance mainly in the settlement joints of the block. For this purpose, two specific test methods were used: thermal camera and infrared thermography. The temperature differences between the internal and external faces were analyzed by means of thermocouples connected in the middle of the prototype and the mapping of the temperature profile on the surface of the cladding. It was found that the addition of gypsum sheathing plus ceramic improves the thermal performance of the masonry system, observing that the variation of the thickness of the gypsum mortar provides a gain in thermal resistance, a reduction in thermal transmittance and an increase in thermal capacity.

Key words: thermal performance; waterproof plaster; thermal camera; infrared thermography; NBR 15220

1. Introduction

In low latitude regions, the presence of high temperatures and humidity causes an increase in the energy consumption of buildings. According to data from EPE (2016), between 1995 and 2014, electricity consumption in Brazil increased by 95%. According to ABRAVA (2016), building systems contribute to the consumption of approximately 50% of the electricity used in Brazil, with a significant portion of this percentage coming from systems dedicated to achieving thermal comfort.

The thermal performance of an environment is related to its thermal load (Çengel, 2007), which is defined as the amount of heat that must be added to or subtracted from an environment to provide a certain desired condition. Inside a building, the following factors are considered determinants of heat load: lighting, number of occupants, and equipment (Souza, 2012). However, in low latitude regions, solar radiation accounts for most of the thermal load inside buildings (Bezerra and Marinho, 2008). According to Azevedo et al. (2016), the reduction of the thermal load inside buildings, which comes in greater proportion from the external environment, can be obtained through the application of thermal insulation, for example, opaque coatings with low thermal conductivity.

The objective of this work is to analyze the thermal behavior of a masonry prototype composed of a solid water-

repellent gypsum block with two types of coatings: gypsum mortar on the internal side and ceramic for the external side. The aim is to make a comparison with the parameters obtained by calculation according to NBR 15220-2 (2005) and NBR 15575-4 (2013) standards, in addition to the experimental analysis of the prototype, by means of infrared thermography, establishing a connection with the values obtained with contact thermocouples.

1.1 The use of gypsum as a thermal insulator

Gypsum has several advantages as a material used for thermal insulation, among them a relatively low cost and a shorter execution time compared to other materials used as cladding, such as Portland cement. In civil construction, it is widely used in the form of blocks in the construction of walls and internal partitions (Peres et al., 2001). In 2015, the Brazilian production of raw gypsum for marketing and processing reached 3.13 Mt, a reduction of 8.5% compared to the previous year, where the state of Pernambuco is the main producer in Brazil, representing 82.5% of the total produced (ANM, 2018). According to Neves (2011), there is an increasing use of this material in multi-story buildings in the large cities of northeastern Brazil and even in the interior, precisely in the states of Pernambuco, Ceará and Sergipe. However, the estimated consumption of gypsum in Brazil is 7 kg/inhabitant/year, which is low compared to Argentina (20 kg/inhabitant/year), Chile (40 kg/inhabitant/year), Japan (80 kg/inhabitant/year), USA (90 kg/inhabitant/year) and Europe (80 kg/inhabitant/year) (FINEP, 2010).

Gypsum is widely used in the production of prefabricated blocks, where they have different characteristics depending on the additive used, being recognized by the color of the block: white - normal, pink - fire resistant (contains fiberglass), green - water resistant (addition of a silicone polymer). Prefabricated blocks can also be used for acoustic insulation (perforated structure) and thermal insulation (addition of an expanded polystyrene plate) (Santos, 2008).

Depending on the location and its characteristics, permeable prefabricated gypsum blocks are used exclusively as internal walls and those with water-repellent characteristics are used in external masonry or in areas with water (Costa and Inojosa, 2007). The latter are known as water-repellent blocks and provide greater thermal insulation (Sobrinho et al., 2010), with a thermal conductivity coefficient equivalent to 0.46 W/°C, indicating a material with thermal insulating properties (Incropera and de Witt, 2003).

Water-repellent gypsum blocks are similar to standard gypsum blocks, except for the addition of a water-repellent additive in their chemical composition. Water-repellent blocks are pigmented by bluish color and are used in the construction of internal and external partitions of wet areas and in the first row of dry areas (PBQP-H, 2017; ITEP, 2007). In Brazil, the water-repellent blocks have a thickness variation of 50, 70 and 100 mm, with a length of 666 mm and a height of 500 mm, presenting a water absorption capacity ≤ 5.0%, defined by the test method described in item 11.5 of NBR 16495 (2016). Table 1 characterizes the water-repellent blocks according to normative criteria.

Table 1. Characteristics of water-repellent gypsum block (NBR 16494, 2017)

Characteristics	Water-repellent block 70	Water-repellent block 100
Thickness, mm	70	100
Type	Massif	Massif
Dimensions, mm	666 × 500	666 × 500
Average weight, kg	24	34
Average weight, kg/m^2	72	102
Surface hardness-solidity (U.S.C.)	≥ 55	≥ 55
Water absorption	< 5%	< 5%
Flexural strength, MPa	≥ 1.2	≥ 1.5

Regarding gypsum for internal coating, it is mainly constituted of calcium sulfate dihydrate, calcined and reduced to powder, being able to have additions or additives in some cases (NBR 16494, 2017). Its use as a coating in indoor environments has several advantages compared to other materials. These advantages include thermal and acoustic insulation, watertightness, fire insulation, wear resistance, regularization of surfaces and base for decorative finishes (Carasek, 2008). Gypsum has a low thermal conductivity coefficient compared to other materials, ranging from 0.25 to 0.50 W/(m °C), this is due to the density of the material, which presents large voids in the intercrystalline spaces (Dias and Cincotto, 1998; Peres et al., 2008).

1.2 Infrared thermography and thermal camera tests

Infrared thermography is a test that measures the radiation emitted by the surface of an object, which is based on the disturbance of heat flow, generated naturally or artificially (Kylili et al., 2014). This causes deviations in the temperature distribution of the object's surface, captured by the thermographic equipment, generating a temperature image, known as a thermogram (Lourenço et al., 2017). The heat flow is responsible for the temperature differences in the thermogram, which depends on the exposure condition of the studied element (Bauer et al., 2015). Infrared thermography is used in various engineering areas for equipment and process monitoring, defect detection and thermal performance studies (Bagavathiappan et al., 2013; Rehman et al., 2016; Lucchi, 2019; O'Grady et al., 2017; Fox et al., 2016).

In the thermal chamber test, temperature is collected through thermocouples placed on the object. In the chamber, there is a heat source that provides the thermal energy that is detected by the thermocouples (Kylili et al., 2014). All the walls of a thermal chamber in the heated environment must be lined with insulating material of the necessary thickness to prevent heat loss to the external environment of the chamber during the test, since the external temperature is always lower than the heated environment inside the chamber. In order to control the external environment, it is necessary to control the climate of the environment, aiming to maintain a temperature outside the thermal chamber close to 26°C. Several results have been obtained in recent researches using thermal chambers in plasterboard masonry (da Silva et al., 2013; Ferreira et al., 2016).

2. Methodology

To achieve the objective of this study, first, a masonry prototype was made with a solid waterproof gypsum block called GH 100+, where: GH is the acronym for waterproof gypsum, 100 is the thickness in millimeters and + is the indication of solids. Subsequently, it was clad with ceramic to simulate the external side and with gypsum of different thicknesses, 0.5 and 1.0 cm, to simulate the internal side of a masonry. Batista (2019) has already experimentally developed a similar prototype with water-repellent gypsum blocks.

The hydrophobic gypsum block was used and it is a material that has replaced traditional technologies such as concrete and ceramic blocks for masonry. This is due to the advantages it offers, such as shorter execution time, design flexibility, better thermoacoustic performance, comfort, among others (Santana et al., 2019). NBR 16494 (2017) provides characteristics (Table 1) and guidelines for the use of water-repellent gypsum blocks in vertical masonry.

Considering that, the highest energy consumption occurs in regions with presence of high temperatures and humidity, Bioclimatic Zone 8 according to NBR 15220-3 (2005), ceramic was used as external cladding. Furthermore, in these regions, the use of ceramic as external coating is quite common (Costa and Silva, 2001). Regarding the plaster coating, NBR 13867 (1997) does not recommend a specific thickness; however, several authors recommend different thicknesses in the range of 0.1 to 1.0 cm, values that depend on the work to be performed (Rocha et al., 2004; Yazigi, 2006; Maeda and Souza, 2003). In this sense, it was decided to analyze two thicknesses of gypsum, 0.5 and 1.0 cm. For the study of its thermal behavior, it was placed in a thermal chamber for heating and a thermographic camera was used to verify the

temperature distribution along the prototype. Finally, the thermal parameters were calculated according to NBR 15220-2 (2005).

2.1 Prototyping

First, it was necessary to prepare the 100 mm thick solid gypsum block (GH 100+), where the cutting regions were demarcated, as shown in Figure 1a, for the production of a 42 × 42 cm^2 vertical masonry prototype. Three blocks were cut, two of 21 × 21 cm^2 and one of 42 × 21 cm^2. The cuts were made to leave male-female ends, allowing the pieces to be glued with glue plaster (Figure 1b). According to Souza (2009), the gypsum glue has a tensile strength superior to the block, providing excellent adhesion and perfect bonding of the parts.

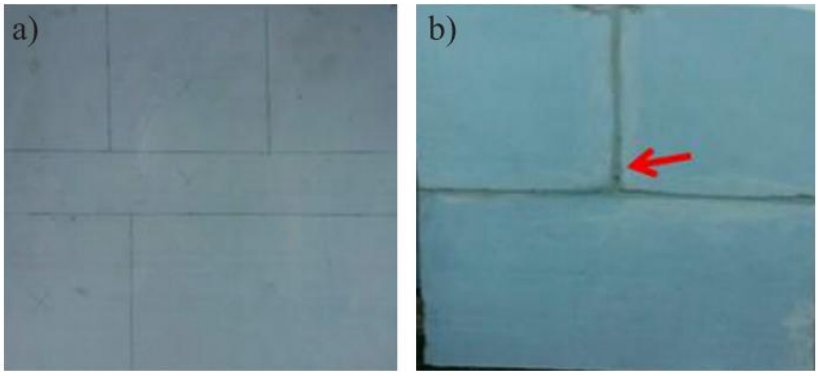

Figure 1. Prototype GH 100+, a) marking of the cuts for the prototype and b) assembly of the 42 × 42 cm^2 prototype, highlighting the joint with the red arrow.

2.2 Execution of the coating

The second stage of the research development consisted of the application of two coatings: 10 × 10 cm^2 ceramic plates (simulating the exterior) and 2-layer gypsum (simulating the interior), each 0.5 cm thick. For the ceramic tiling, Weber (2018) recommends the use of adhesives or other glues that do not contain Portland cement for the placement of the ceramic slabs on the gypsum block. In this research, gypsum glue was used in the ratio of 1 kg/700 ml of water, as recommended by the manufacturer. After 7 days of placement, the grout was applied and waited more than 15 days to avoid the appearance of cracks during the heating of the system (Figure 2a).

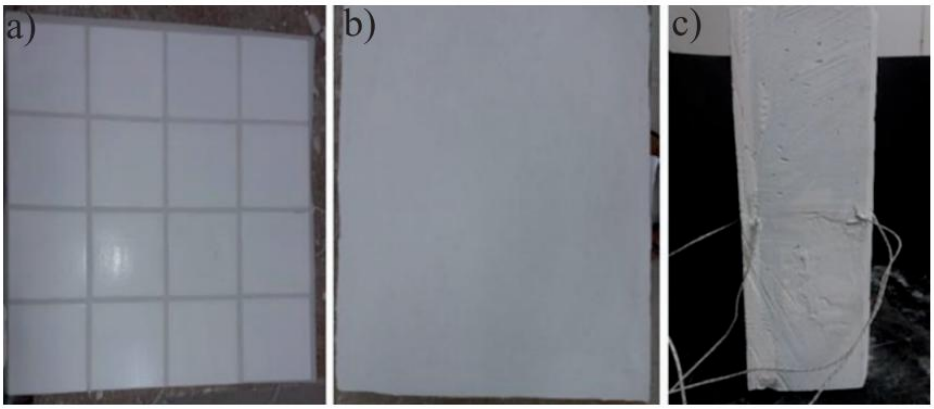

Figure 2. Prototype of the masonry: a) ceramic coating, b) plaster coating and c) vertical cut of the prototype.

The gypsum coating was applied in two layers to achieve thicknesses of 0.5 and 1.0 cm (Figure 2b). After the execution of the first layer, a period of 7 days was waited to verify the thermal behavior of the prototype. Then the second layer was applied and another 7 days were waited for the second verification. Figure 2c shows the positioning of the two coatings, with the ceramic tile on the right and the plaster on the left. In the middle is the GH 100+ masonry.

2.3 Thermal chamber test

For the thermal behavior verification test, a thermal chamber with dimensions of 43 × 40 × 43 cm^3 was used (Figure 3). The heat source was a 250 W lamp located in the central region of the interior, 11.5 cm from the test element. For data collection purposes (temperature), two thermocouples were applied to the inside (hot side) and outside (cold side) of the chamber. The control measure imposed was the thermal regulation of the external environment, making it possible to simulate a colder climate, around 26°C.

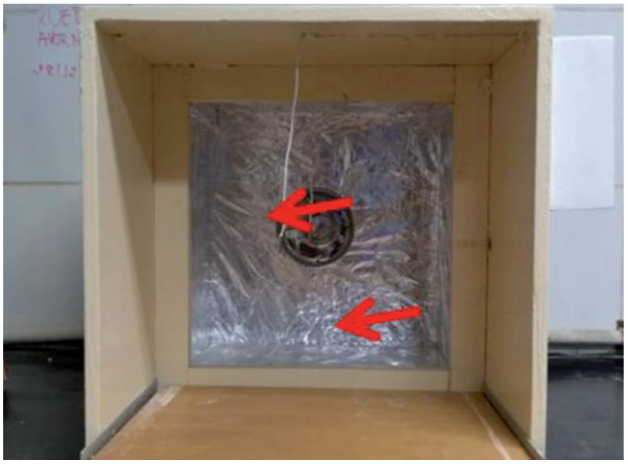

Figure 3. Thermal camera with lamp, highlighting with arrows the heat source and thermocouple.

According to Silva et al. (2012), to obtain more representative data, the location of the thermocouple should be in the center of the object under study, where it receives a higher concentration of heat from the thermal source. For this research, it was chosen to place the thermocouples in the center of the prototype, one on the side exposed to heat (hot side) and the other on the opposite side (cold side), fixed by metal straps. To measure the heating temperature, the thermocouples were connected to a four-channel digital thermometer MT-1044 - MINIPA® programmed to record values at one-minute intervals. The test had a duration of 6 hours.

Figure 4a indicates the direction of the heat flow acting on the hot side, composed of the ceramic lining, and on the cold side, composed of the gypsum lining, following a model similar to that of da Silva et al. (2013). The masonry prototype and verification of the performance of the masonry system similar to Ferreira et al. (2016) were used. Figure 4b shows the prototype after the application of the coatings and ready for testing. It is possible to identify the location of the thermocouples in the center of the prototype.

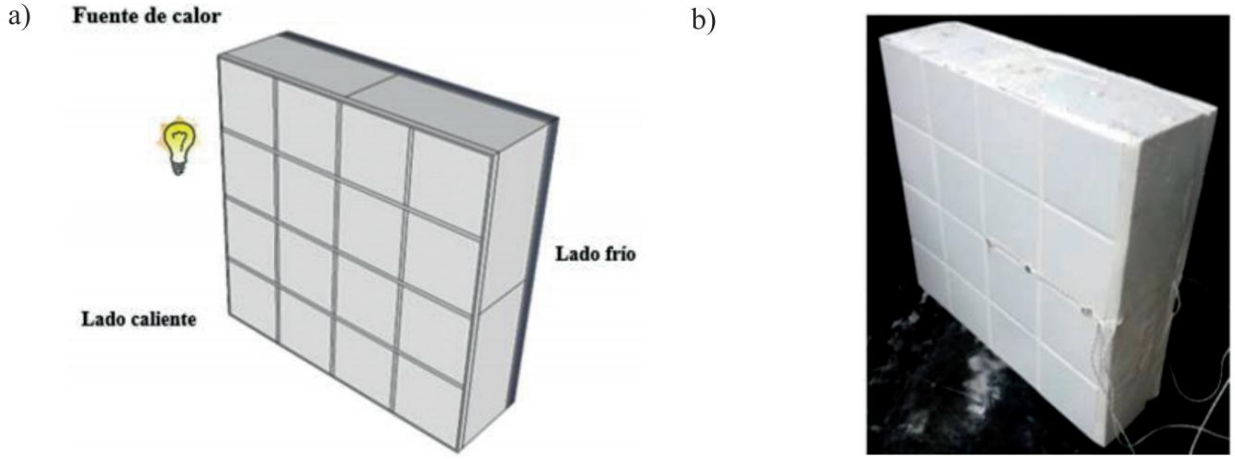

Figure 4. Schematic model of the prototype: a) indication of the heat source and b) location of the thermocouples.

To facilitate the understanding of the analysis, the nomenclature was adopted according to the order of the test:

Case 1: uncoated prototype (Figure 5a);

Case 2: prototype with ceramic coating on the hot side and 0.5 cm of gypsum coating on the cold side (Figure 5b);

Case 3: prototype with ceramic coating on the hot side and 1.0 cm of gypsum coating on the cold side (Figure 5c).

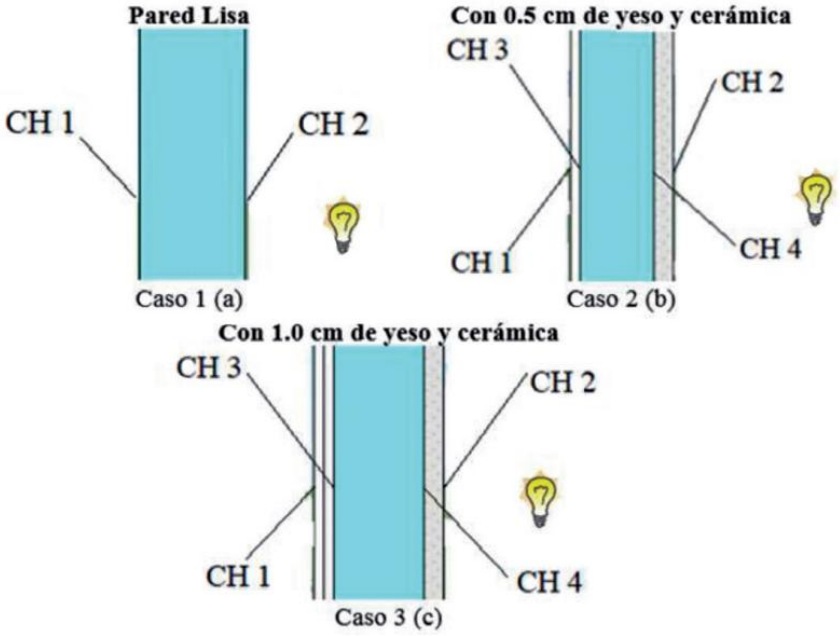

Figure 5. Order of tests, position of thermocouples and indication of the location of the heat source for: a) Case 1, b) Case 2 and c) Case 3.

As for the thermocouples, CH 1 and CH 3 were located on the cold side, while CH 2 and CH 4 thermocouples were located on the hot side (Figure 5). The general nomenclature is detailed in Table 2.

Table 2. Summary of thermocouple positions

Cases	Thermocouple used	Meaning
1	CH 1	Cold side
	CH 2	Hot side
2	CH 1	Cold side (over plaster lining)
	CH 2	Hot side (on the ceramic coating)
	CH 3	Cold side (between gypsum sheathing and GH 100+ block)
	CH 4	Hot side (between the ceramic lining and the GH 100+ block)
3	CH 1	Cold side (over plaster lining)
	CH 2	Hot side (on the ceramic coating)
	CH 3	Cold side (between gypsum sheathing and GH 100+ block)
	CH 4	Hot side (between the ceramic lining and the GH 100+ block)

2.4 Temperature along the prototype using infrared thermography

Heating of the prototype was accompanied with a thermographic camera at one-hour intervals. During heating, thermograms were taken only from the outside of the thermal chamber (cold side). The cooling process was recorded after removing the prototype from the thermal chamber, where thermograms were generated at 30-min intervals. For this

purpose, a FLIR thermographic camera, model E60, was used. The thermograms obtained were processed by assigning a color to each temperature (Usamentiaga et al., 2014). Careful selection of the emissivity value was necessary to simplify the interpretation of the thermal image (Barreira et al., 2017). According to Incropera and de Witt (2003), the emissivity value varies according to the type of material, and there are several possible test methods, such as the black tape method (Lourenço et al., 2017). For this research, the emissivity values obtained for plaster and ceramic tiles were 0.95 and 0.87, respectively. Through these values, the thermal images were adjusted using FLIR TOOLS® software, where the range from 23°C (lowest temperature) to 39°C (highest temperature) was used to improve the difference between the thermograms taken.

2.5 Calculation of thermal parameters

To calculate the thermal parameters of the masonry system, the method presented in NBR 15220-2 (2005) was used, where most of the input data were obtained: thermal conductivity, specific heat and bulk density of the materials used. The bulk density of the materials was determined in the laboratory using samples taken from the available stock. Table 3 shows the values obtained.

Table 3. Data on materials used

Material	Thermal conductivity, W/(mK)	Specific heat, kJ/(kgK)	Bulk density, kg/m^3
GH 100+ plate	0.35	0.84	1084
Ceramics	1.05	0.92	3000
Board	1.15	1.00	1980
Plaster coating	0.70	0.84	1100

3. Analysis of Results

3.1 Temperature of the prototype during the test in the thermal chamber

From the results presented in Table 4, it is evident that, on the cold side of the prototype, up to a period of one hour, it did not present significant changes in relation to temperature. Case 3 CH 3 presented a variation of 1.4°C in this interval. However, after 2 hours, there was a growth of the same amount. Case 1 showed the highest temperature variation, around 9.5°C in the 6-hour period of the test, while Cases 2 and 3 presented a reduction of 7°C (22%) and 6.5°C (28%) in comparison with Case 1. When comparing the CH 3 thermocouple in Cases 2 and 3, a reduction of 1.0°C and 0.5°C, respectively, was observed in relation to the CH 1 thermocouple of Case 1. Cases 2 and 3 showed a difference of 0.5°C relative to the CH 3 thermocouple, probably due to the climate-controlled conditions of the environment, which caused this difference in the cold-side temperature variation during the heating test.

Table 4. Temperature variation at each hour in relation to the heating of the cold side of the prototype

Time hh:mm	Temperature, °C				
	Case 1 CH 1	Case 2 CH 1	Case 2 CH 3	Case 3 CH 1	Case 3 CH 3
00:00	26.3	26.8	27.3	25.8	25.7
01:00	27.0	26.9	27.4	26.7	27.1
02:00	29.9	28.5	29.3	27.8	28.6
03:00	31.8	30.3	31.4	29.4	30.6
04:00	33.4	31.6	33.0	30.7	32.3
05:00	34.6	32.7	34.3	31.7	33.7

Time hh:mm	Temperature, °C				
	Case 1 CH 1	Case 2 CH 1	Case 2 CH 3	Case 3 CH 1	Case 3 CH 3
06:00	35.8	33.8	35.8	32.3	34.7
Variation	9.5	7.0	8.5	6.5	9.0

Figure 6 shows the evolution of the heating of the cold side, where it is possible to observe the variation in the behavior of the prototype according to the presence of the coatings. In the first hour, the temperature did not vary much, but after this period, there is a growth of the same. It was observed that after completing 6 hrs of the test, the average temperature on the cold side reached the maximum value. Case 1 showed the highest temperature growth in the region near the block joint, considering that this region is a critical point for thermal comfort (Poças, 2008). In Cases 2, CH 1 and 3 CH 1, an improvement can be perceived, according to the behavior shown in Figure 6, indicating a reduction of approximately 2°C after 6 hrs compared to Case 1. Compared to Case 1 Ch1, Cases 2 Ch3 and Case 3 Ch3 exhibit similar behavior.

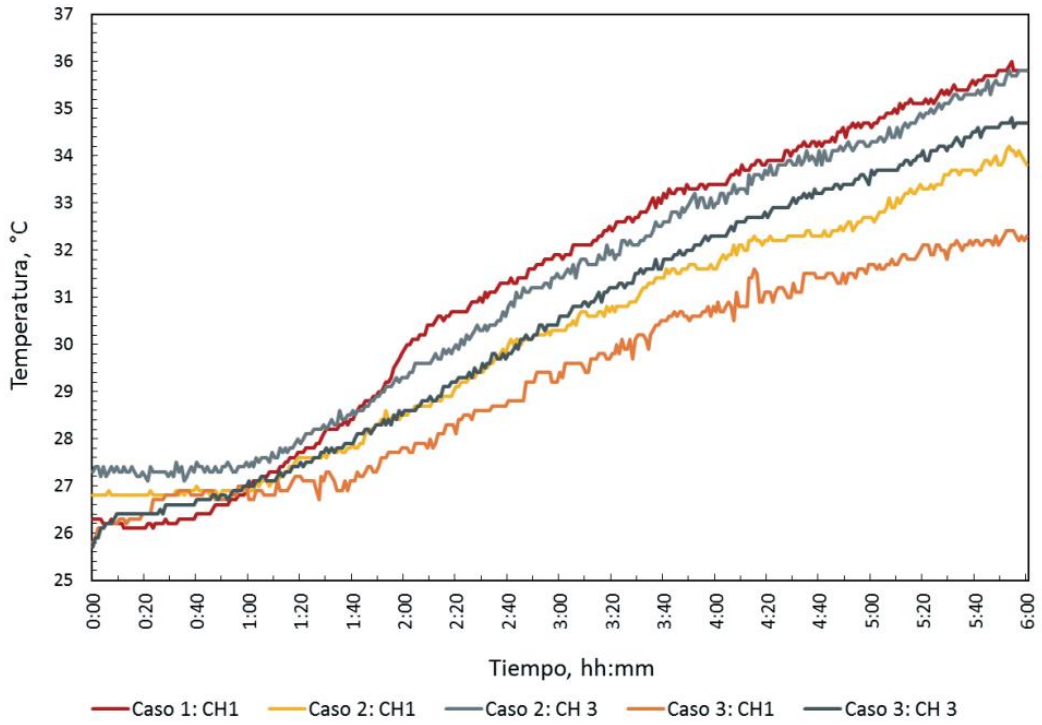

Figure 6. Temperature variation in cold side heating.

The temperature variation on the cold side can be explained by the heat transfer in the system. On the external (ceramic) side, there is heating by convection with the air and radiation by the 250 W lamp. Part of the radiation is reflected and part is absorbed; the transmission is zero, since the analyzed prototype is an opaque body. The absorbed radiation is conducted through the prototype through heating, as shown in Figure 6. The heating takes a period of about one hour to influence the temperature of the cold side. In Case 1, the heat transfer is direct. However, the presence of ceramic (Cases 2 and 3) interrupts the direct heat transfer, since the ceramic has different thermal conductivity (Table 3) and, for the same time and thermal load, the temperatures are lower (CH 3) than Case 1 (CH 1), Figure 6 and Table 4. And for the gypsum lining, the heat transfer by conduction is limited by each layer of gypsum added, so the surface temperature of Case 3 (CH 1) is lower than Case 2 (CH 2).

Table 5 shows the cooling behavior of the prototype on the cold side. It is worth noting that, after turning off the heat source, it took about 30 minutes to reduce the temperature. At around 2 hrs, according to the CH 1 thermocouple, Case 1 suffered a heat loss of 3°C, and for Case 2, there was a reduction of 1.2°C. In Case 3, there was a reduction of 1.1°C. These results indicate that there was a 60% reduction in heat loss for Case 2 and 63% for Case 3, which represents a considerable gain in comfort. It should also be noted that for thermocouple CH 3, the reduction was 1.6°C in both cases.

Table 5. Half-hourly temperature variation in relation to the cooling of the cold side of the prototype

Time hh:mm	Temperature, °C				
	Case 1 CH 1	Case 2 CH 1	Case 2 CH 3	Case 3 CH 1	Case 3 CH 3
00:00	35.9	33.9	35.7	32.3	34.8
00:30	36.7	34.4	36.1	32.3	35.0
01:00	35.9	34.4	36.2	32.7	34.9
01:30	34.7	33.6	35.0	32.0	34.0
02:00	32.9	32.7	34.1	31.2	33.2
Variation	-3.0	-1.2	-1.6	-1.1	-1.6

Once the heat source is turned off, the heat transfer process continues for approximately 30 min (Figure 7). It is observed that the cooling behavior for the analyzed cases was similar, noting that Case 1 lost heat faster, stabilizing around 32°C, while for Cases 2 and 3, upon analyzing the CH 1 thermocouple, it is observed that the heat loss is small, especially for Case 3, which is probably due to the presence of a 1 cm thick gypsum cover.

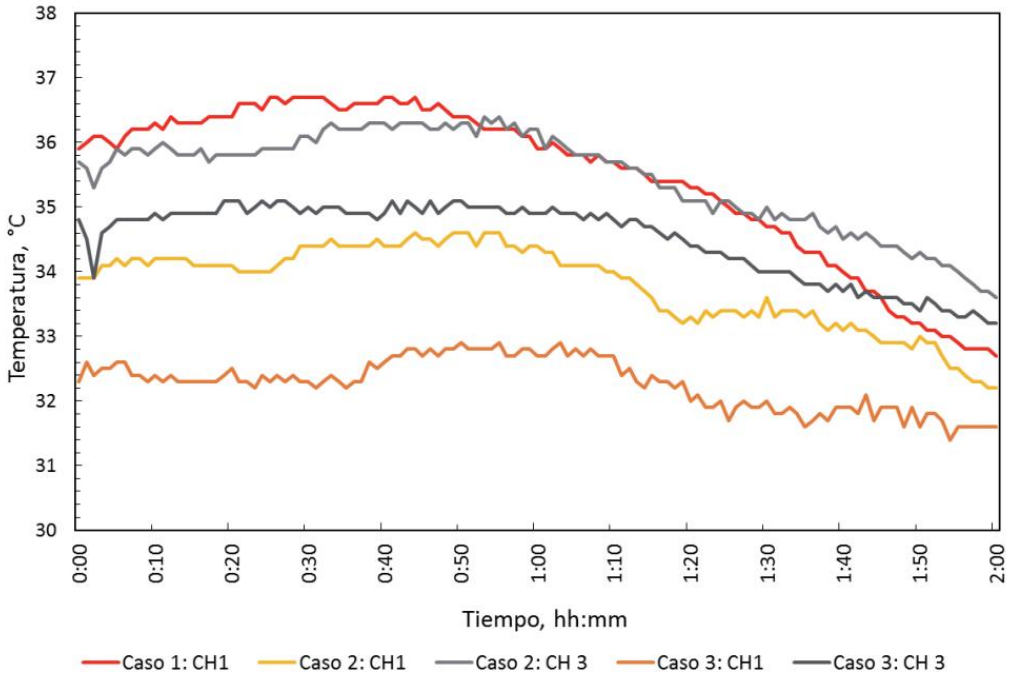

Figure 7. Cooling of the cold side of the prototype in relation to analysis time.

This behavior is due to the thermal equilibrium with the environment by the convection mechanism. The external surface heated by the 250 W lamp emits radiation heating the environment of the thermal box, which prevents the temperature from dropping rapidly. The heat is maintained for a period of 30 minutes. On the cold side, the behavior is different between Case 1 and Cases 2 and 3. In Case 1 CH 1, the variation is higher, this is due to the fact that the prototype

only consists of the GH 100+ block, therefore, the thermal equilibrium by convection with the environment takes place faster; indicating higher thermal diffusivity (temperature variation speed) than the other systems, since the GH 100+ block has higher thermal conductivity and lower specific heat (Table 3). In Cases 2 and 3 for CH 1, the variation is similar. This similarity is due to the same coating material. The convective thermal equilibrium with the environment is similar in time. For CH 3 of Cases 2 and 3, the variation is the same, since the heat transfer by conduction on the hot side is the same, involving the GH 100+ block and ceramic material.

3.2 Temperature of the prototype by infrared thermography

Thermogram analysis shows the heating process during the 6-hour test interval for the cold side (Figures 8, 9 and 10). The thermal scale was adjusted between 23 and 39°C to allow comparison between tests. For Case 1, it was possible to note that in the first hour, there was a significant variation in hue, intensified by heat transfer, being that the lighter the color, the higher the temperature. The heat distribution was from the central region to the edges (Figures 8a and 8b). After 2 hrs (Figure 8c), light colors are observed at the edges, more intense at the top, in the direction of the settlement of the block, which probably indicates the direct influence on the heat distribution at this point. Consequently, with the passage of time, there was an expansion of this region accentuating in a round shape, concentrating much of the energy transferred from the heat source to the central part (Figures 8d, 8e and 8f). At the end of the 6 hrs of heating, it is worth noting that the heat distribution tends to occupy the regions of the settlement joint, moving from the center to the left and right edges of the middle upwards (Figure 8g), indicating a possible critical region for the thermal comfort of masonry in solid waterproof plaster.

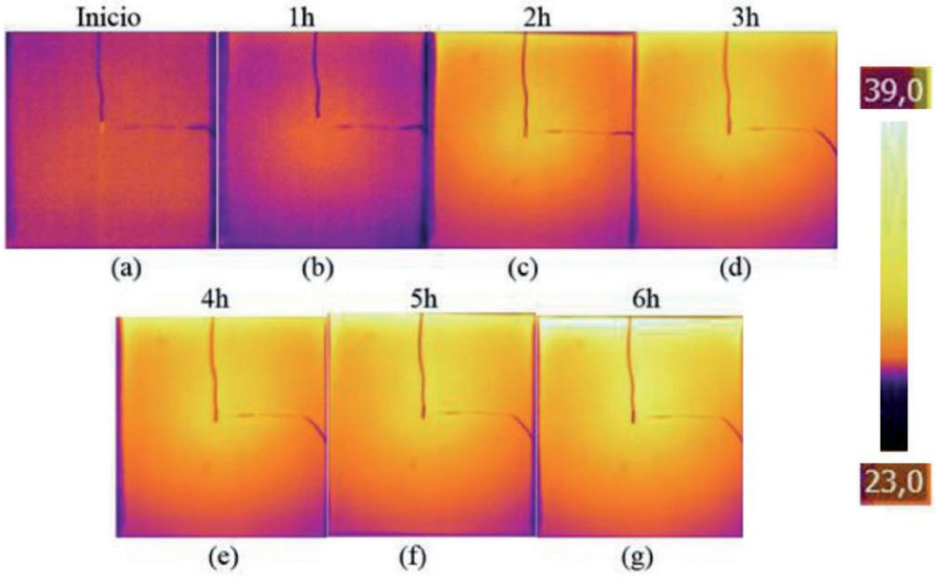

Figure 8. Thermograms of cold side heating, Case 1, for times in hours: a) 0, b) 1, c) 2, d) 3, e) 4, f) 5 and g) 6.

The thermograms of Case 2 had a lower intensity of the tone, lighter compared to Case 1. It is observed that the prototype started to change the tone in the central region from 2 hrs after the start of the test, unlike Case 1 (Figures 9a, 9b and 9c). After this period, a slight variation of the shade and uniformity of the light shade distribution of the surface can be observed, indicating a possible improvement in the distribution of heat transferred from the hot source and that the gypsum coating is a possible correction for the problem presented in Case 1, indicating an improvement in the thermal performance of the prototype. Comparing the final interval at 6 hrs of testing (Figures 8g and 9g), it is observed that less heat has passed through.

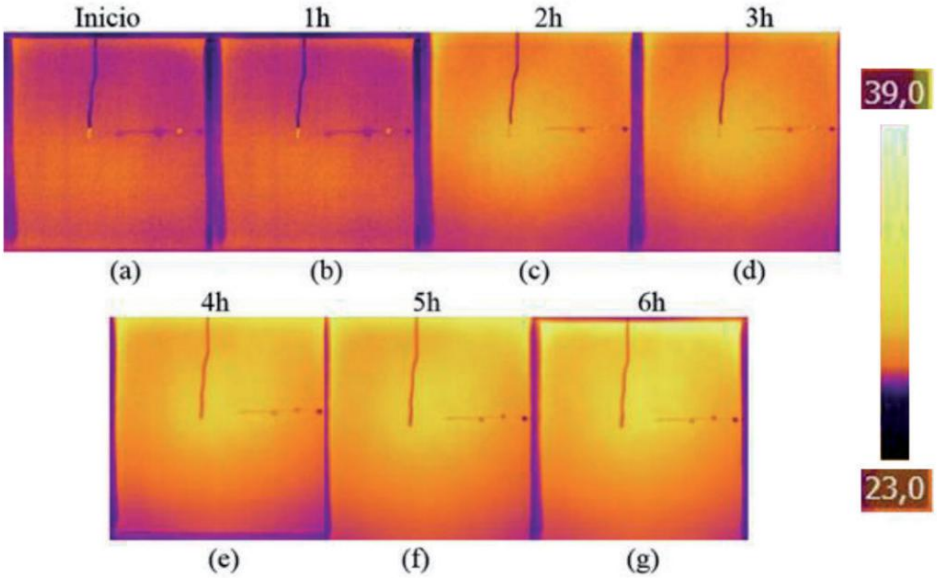

Figure 9. Thermograms of cold side heating, Case 2, for times in hours: a) 0, b) 1, c) 2, d) 3, e) 4, f) 5 and g) 6.

With respect to Case 3, a reduction in hue was observed compared to Case 2. The prototype began to show a color change in the central region 2 hrs after the start of the test, indicating an improvement with respect to Case 1 (Figures 10a, 10b and 10c). After this period (Figure 10d), it is observed that the heat distribution on the surface is more uniform and less intense than that of Case 2, indicating that the increase in the thickness of the coating contributes to improve the thermal performance of the masonry by increasing the thermal resistance (Table 6). When comparing the final interval for Cases 1, 2 and 3 after 6 hrs of testing (Figures 8g, 9g and 10g), it was observed that, with the same thermal load and exposure interval, the prototype that presented better performance was Case 3.

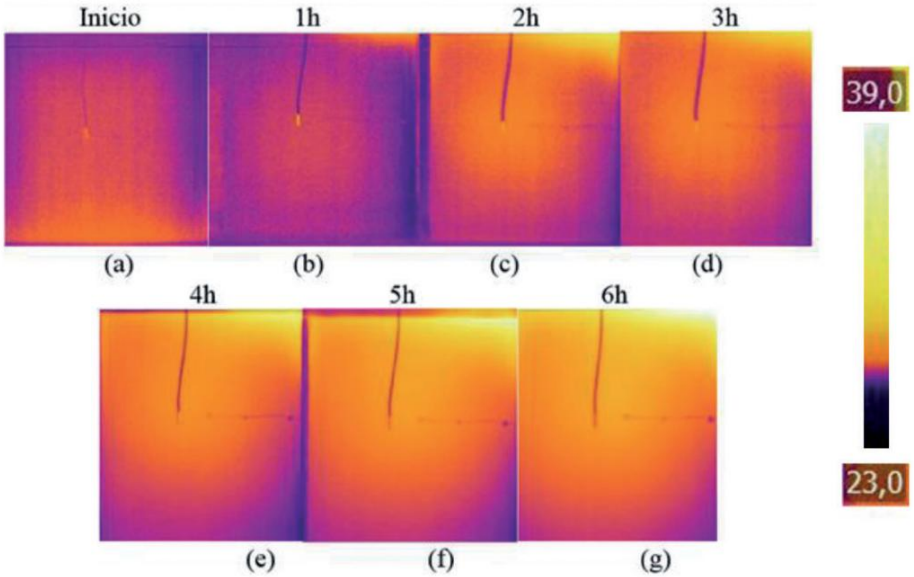

Figure 10. Thermograms of cold side heating, Case 3, for times in hours: a) 0, b) 1, c) 2, d) 3, e) 4, f) 5, and g) 6.

As can be seen in the three cases presented, the highest temperatures are in the central part of the prototype, indicating that the heating is mainly due to the radiation absorbed by the 250 W lamp rather than to convection with the air inside the prototype. Although it is also observed, in later hours, that the upper part of the prototype presents higher temperature than

the lower part, this is due to heat transfer by convection, since the hot fluids (air) move upwards, due to the increase in volume (lower density). From the thermograms presented, the heating in the prototype can be qualitatively appreciated, verifying the thermal diffusivity of each system. As explained in the previous subheading, the highest thermal diffusivity corresponds to Case 1 and the lowest to Case 3.

3.3 Analysis of the calculation of thermal parameters

Table 6 shows the values obtained for the thermal parameters, according to NBR 15220-2 (2005), for the prototype with the different cladding configurations (Cases 1, 2 and 3).

Table 6. Total thermal resistance, thermal transmittance, thermal capacity and thermal delay for the cases studied

Cases	Total thermal resistance, m^2K/W	Thermal transmittance, $W/(m^2K)$	Heat capacity, $kJ/(m^2K)$	Thermal lag, hours
Case 1	0.46	2.19	91.06	3.72
Case 2	0.47	2.14	108.78	3.75
Case 3	0.48	2.11	113.82	3.79

According to NBR 15220-2 (2005), the higher the thermal resistance, the better the thermal performance of the system. For the cases with the addition of coating, a gain in thermal resistance over the prototype without the presence of coating can be observed. Case 2 presented the value of 0.47 m^2K/W, which corresponds to an increase of 2.41% compared to Case 1, and Case 3 presented the value of 0.48 m^2K/W, which is equivalent to a gain of 4.17% over Case 1, i.e., the prototype with greater coating thickness resists thermal flow better.

With respect to thermal transmittance, the lower the value of this parameter, the better the thermal performance of the component, since the heat flow through it will be lower. Case 2 presents a value of 2.14 $W/(m^2K)$, which represents a reduction of 2.41% compared to Case 1, and 2.11 $W/(m^2K)$ for Case 3, equivalent to a reduction of 4.17%, with the latter presenting better thermal performance. The transmittance values are below 2.5 $W/(m^2K)$ presenting performance in relation to the external walls according to item 11.2.1 of NBR 15575-4 (2013).

The thermal capacity represents the amount of heat required to vary by 1°C in a given system. It can be noted that Case 2 obtained a value of 108.78 $kJ/(m^2K)$, which represents an increase of 19.4% compared to Case 1, and Case 3 obtained a value of 113.82 $kJ/(m^2K)$, which represents a gain of 25% compared to Case 1. The values presented for thermal capacity are below 130 $kJ/(m^2K)$, not complying with criterion 11.2.2 of NBR 15575-4 (2013).

According to NBR 15220-2 (2015), the thermal lag represents the time required for the thermal action of a medium to manifest itself on the opposite surface, subjected to a periodic heat transfer regime. It was observed that the uncoated prototype (Case 1) had a value of 3.72 hrs, higher than the addition of coatings, which was 3.65 hrs for Case 2, and 3.69 hrs for Case 3. NBR 15220-2 (2005) points out that, in the case of a component formed by different materials superimposed in n layers parallel to the faces (perpendicular to the heat flow), the thermal lag varies according to the order of the layers, which may justify this variation in the thermal lag values with the addition of coatings.

In the present study, the results are limited to one test. It is necessary to perform more tests considering other variables such as repeatability of the data, intermediate thicknesses of gypsum sheathing, different heating sources, among others, in order to be certain of the influence of the sheathing on the thermal behavior of gypsum block masonry; however, the results presented give an idea of the behavior of this, which can serve as a basis for future research.

4. Conclusions

When analyzing the results obtained with the thermal chamber, it was verified that there was a gain in the thermal behavior of the prototype with the presence of the coatings, indicating the reduction of the thermal load transferred and the

consequent gain in thermal comfort. This gain was greater when the thickness of the gypsum sheathing was increased. The influence occurred in both the heating and cooling processes. Additionally, it could be observed that the temperature variation in heating was greater than in cooling due to the elimination of the heat source. The same result was verified when analyzing the thermograms. There was a gain in thermal behavior in relation to the cold side due to the presence of the gypsum coatings.

Regarding the calculations of the thermal parameters, the thermal capacity of the prototype increased by 25% with the application of 1.0 cm of gypsum coating with ceramic compared to the same without coating.

From the results obtained, it can be deduced that solid water-repellent gypsum masonry significantly improves the thermal performance when a gypsum or ceramic coating is applied. However, further research is needed to generalize the conclusions and to ensure the accuracy of the thermal performance of water-repellent gypsum.

Conflicts of Interest

The author declares no conflicts of interest regarding the publication of this paper.

References

[1] ABRAVA. 2016. O consumo de energia elétrica nas edificações do Brasil. Associação Brasileira de Refrigeração, Ar Condicionado, Ventilação e Aquecimento ABRAVA. http://abrava.com.br

[2] ANM. 2018. Sumário mineral 2016. Departamento Nacional da Produção Mineral. Agência Nacional de Mineração. Brasília, Brasil.

[3] Azevedo, C., Santos, I.I. e Marinho, G.S. 2016. Análise de propriedades termofísicas de compósito para isolação térmica. Congresso Nacional de Engenharia Mecânica CONEM, Fortaleza, Brasil.

[4] Bagavathiappan, S., Lahiri, B.B., Saravanan, T., Philip, J. and Jayakumar, T. 2013. Infrared thermography for condition monitoring - A review. *Infrared Physics & Technology*, 60: 35-55.

[5] Barreira, E., Almeida, R.M. and Moreira, M. 2017. An infrared thermography passive approach to assess the effect of leakage point in buildings. *Energy and Buildings*, 140: 224-235.

[6] Batista, P. 2019. Parâmetros de desempenho térmico de blocos de gesso. MSc. thesis, Escola Politécnica de Pernambuco, Recife, Brasil.

[7] Bauer, E., Castro, E.K., Pavon, E. and Oliveira, A.H. 2015. Criteria for application and identification of anomalies on the facades of buildings with the use of passive infrared thermography. 1st International Symposium on Building Pathology. Porto, Portugal.

[8] Bezerra, L.A. e Marinho, G.S. 2008. Elementos de alvenaria termo-isolante produzidos com poliestireno expandido reciclado. *Mens Agitat*, 3(2): 17-26.

[9] Carasek, H. 2007. Argamassas. Materiais de Construção Civil e Princípios de Ciência e Engenharia de Materiais. Isaia, G.C. (ed.). Instituto Brasileiro do Concreto IBRACON. São Paulo, Brasil.

[10] Çengel, Y.A. 2007. Heat and mass transfer: A practical approach. 3rd edition. McGraw-Hill, New York, USA.

[11] Costa, A.M. e Inojosa, A.C. 2007. Alvenaria em blocos de gesso. Sistema Construtivo Gypway. Sindicato da Indústria do Gesso SINDUSGESSO, Brasil.

[12] Costa e Silva, A.J. 2001. Descolamentos dos revestimentos cerâmicos de fachada na cidade do Recife. MSc thesis, Universidade de São Paulo, Brasil.

[13] da Silva, E.P., de Melo, A.B. e Queiroga, A.B. 2013. Desempenho térmico de vedações: estudo comparativo com blocos de EVA, tijolo cerâmico e gesso acartonado. XII ENCAC-Encontro Nacional de Conforto no Ambiente Construído e VIII ELACAC-Encontro Latinoamericano de Conforto no Ambiente Construído. Brasília, Brasil.

[14] Dias, A. e Cincotto, M. 1995. Revestimento à base de gesso de construção. Boletim Técnico 142. EPUSP. São Paulo, Brasil.

[15] EPE. 2016. Consumo nacional de energía: 1995-2014. Empresa de Pesquisa Energética EPE. Rio de Janeiro, Brasil.

[16] Ferreira, P.R., Henriques, V.M., de Melo, A.B. e Gomes, E.G. 2016. Avaliação do comportamento térmico de paredes monolíticas executadas com diferentes materiais em condições variáveis de oscilações de temperaturas superficiais. XVI Encontro Nacional de Tecnologia do Ambiente Construído, São Paulo, Brasil.

[17] FINEP. 2010. Financiadora de estudos e projetos. www.finep.gov.br

[18] Fox, M., Goodhew, S. and Wilde, P. 2016. Building defect detection: External versus internal thermography. *Building and Environment*, 105: 317-331.

[19] Incropera, F.P. e de Witt, D.P. 2003. Fundamentos de transferência de calor e de massa. 4ª edição. Guanabara Koogan, Rio de Janeiro, Brasil.

[20] ITEP. 2007. Casas térreas em paredes de alvenaria em blocos de gesso. Manual Construtivo. Recomendações Técnicas ITEP. Recife, Brasil.

[21] Kylili, A., Fokaides, P.A., Christou, P. and Kalogirou, S.A. 2014. Infrared thermography (IRT) applications for building diagnostics: a review. *Applied Energy*, 134: 531-549.

[22] Lourenço, T., Matias, L. and Faria, P. 2017. Anomalies detection in adhesive wall tiling systems by infrared thermography. *Construction and Building Materials*, 148: 419-428.

[23] Lucchi, E. 2018. Applications of the infrared thermography in the energy audit of buildings: A review. *Renewable and Sustainable Energy Reviews*. 82: 3077-3090.

[24] Maeda, F.M. e Souza, U.E.L. 2003. Previsão da produtividade da mão-de-obra na execução de revestimento interno em gesso. Boletim técnico 332. EPUSP. São Paulo, Brasil.

[25] NBR 13867. 1997. Revestimento interno de paredes e tetos com pasta de gesso - Materiais, preparo, aplicação e acabamento. Associação Brasileira de Normas Técnicas ABNT, Rio de Janeiro, Brasil.

[26] NBR 15220-2. 2005. Desempenho térmico de edificações. Parte 2: Método de cálculo da transmitância térmica, da capacidade térmica, do atraso térmico e do fator solar de elementos e componentes construtivos. Associação Brasileira de Normas Técnicas ABNT, Rio de Janeiro, Brasil.

[27] NBR 15220-3. 2005. Desempenho térmico de edificações. Parte 3: Zoneamento bioclimático brasileiro e diretrizes construtivas para habitações unifamiliares de interesse social. Associação Brasileira de Normas Técnicas ABNT, Rio de Janeiro, Brasil.

[28] NBR 15575-4. 2013. Edifícios habitacionais - Requisitos para sistema de vedação vertical interna e externa - SVVIE. Associação Brasileira de Normas Técnicas ABNT. Rio de Janeiro, Brasil.

[29] NBR 16494. 2017. Bloco de gesso para vedação vertical - Requisitos. Associação Brasileira de Normas Técnicas ABNT, Rio de Janeiro, Brasil.

[30] NBR 16495. 2016. Bloco de gesso para vedação vertical - Método de ensaio. Associação Brasileira de Normas Técnicas ABNT, Rio de Janeiro, Brasil.

[31] Neves, M.L. 2011. Método construtivo de vedação vertical interna com blocos de gesso. MSc thesis, *Escola Politécnica de Pernambuco*, Recife, Brasil.

[32] O'Grady, M., Lechowska, A.A. and Harte, A.M. 2017. Infrared thermography technique as an in-situ method of assessing heat loss through thermal bridging. *Energy and Buildings*, 135: 20-32.

[33] PBQP-H. 2017. Programa Brasileiro da qualidade e produtividade do habitat. Sistema Nacional de Avaliações Técnicas SINAT. Brasilia, Brasil. http://pbqp-h.mdr.gov.br/projetos_sinat.php

[34] Peres, L., Benachour, M. e Santos, V.A. 2008. Gesso: produção e utilização na construção civil. Sebrae, Recife, Brasil.

[35] Peres, L.M., Benachour, M. e Santos, V.A. 2001. O Gesso: produção e utilização na construção civil. Bagaço, Recife, Brasil.

[36] Poças, J.P. 2008. Estudo do comportamento térmico e mecânico em paredes de alvenaria. MSc thesis, Universidade do Porto, Portugal.

[37] Rehman, S.K.U., Ibrahim, Z., Memon, S.A. and Jameel, M. 2016. Nondestructive test methods for concrete bridges: A review. *Construction and Building Materials*, 107: 58-86.

[38] Rocha, E., Medeiros, E., Gabriel, F., Uchôa, J., Marlo, J., Santos, L. e Medeiros, P. 2004. Sistemas de revestimentos - Diagnóstico Local - Brasília/DF. Universidade de Brasília, Brasil.

[39] Santana, C.V.D., Póvoas, Y.V., Silva, D.G.C.D. and Miranda Neto, F.D.A. 2019. Recycled gypsum block: development and performance. *Ambiente Construído*, 19(2): 45-58.

[40] Santos, R. 2008. Estudo térmico e de materiais de um composto a base de gesso e EPS para construção de casas populares. MSc thesis, Universidade Federal de Rio Grande do Norte, Natal, Brasil.

[41] Silva, E.P., Cahino, J.E. e Melo, A.B. 2012. Avaliação do desempenho térmico de blocos EVA. Encontro Nacional de Tecnologia do Ambiente Construído, Juiz de Fora, Brasil.

[42] Sobrinho, C.W.A.P., Bezerra, N.M., Costa, T.C.T. e Silva, C.B.A.S. 2010. Divisórias internas de edifícios em alvenaria de blocos de gesso - Vantagens técnicas, econômicas e ambientais. Congresso Internacional de Tecnologia Aplicada para a Arquitetura e Engenharia Sustentáveis. Recife, Pernambuco, Brasil.

[43] Souza, A.C. 2009. Análise comparativa de custos de alternativas tecnológicas para construção de habitações populares. MSc thesis, Universidade Católica de Pernambuco, Recife, Brasil.

[44] Souza, V.A. 2012. Estudo do comportamento de materiais não convencionais utilizados como revestimentos de parede, visando à redução da carga térmica. MSc thesis, Universidade Federal da Paraíba, João Pessoa, Brasil.

[45] Usamentiaga, R., Venegas, P., Guerediaga, J., Vega, L., Molleda, J. and Bulnes, F.G. 2014. Infrared thermography for temperature measurement and non-destructive testing. *Sensors*, 14(7): 12305-12348.

[46] Weber. 2018. Colagem de cerâmica sobre suportes de gesso em interior. https://www.weber.com.pt/colagem-e-betumacao-de-ceramica

[47] Yazigi, W. 2006. A técnica de edificar. 6ª ed. Pini. São Paulo, Brasil.